Journal of
PERIODONTAL RESEARCH

J Periodont Res 2011; 46: 682–690

JOURNAL OF PERIODONTAL RESEARCH
doi:10.1111/j.1600-0765.2011.01390.x

Induction of bone formation by *Escherichia coli*-expressed recombinant human bone morphogenetic protein-2 using block-type macroporous biphasic calcium phosphate in orthotopic and ectopic rat models

J-C. Park[1]*, S-S. So[1]*, I-H. Jung[1], J-H. Yun[2], S-H. Choi[1], K-S. Cho[1], C-S. Kim[1]

[1]Department of Periodontology, Research Institute for Periodontal Regeneration, College of Dentistry, Yonsei University, Seoul, South Korea and [2]Division of Periodontology, Department of Dentistry, School of Medicine, Inha University, Incheon, South Korea

Park J-C, So S-S, Jung I-H, Yun J-H, Choi S-H, Cho K-S, Kim C-S. Induction of bone formation by Escherichia coli*-expressed recombinant human bone morphogenetic protein-2 using block-type macroporous biphasic calcium phosphate in orthotopic and ectopic rat models. J Periodont Res 2011; 46: 682–690.*

Background and Objective: The potential of the *Escherichia coli*-expressed recombinant human bone morphogenetic protein-2 (ErhBMP-2) to support new bone formation/maturation using a block-type of macroporous biphasic calcium phosphate (bMBCP) carrier was evaluated in an orthotopic and ectopic rat model.

Material and Methods: Critical-size (Φ 8 mm) calvarial defects and subcutaneous pockets in 32 Sprague–Dawley rats received implants of rhBMP-2 (2.5 μg) in a bMBCP carrier or bMBCP alone (control). Implant sites were evaluated using histological and histometric analysis following 2- and 8-wk healing intervals (eight animals/group/interval).

Results: ErhBMP-2/bMBCP supported significantly greater bone formation at 2 and 8 wk (10.8% and 25.4%, respectively) than the control at 2 and 8 wk (5.3% and 14.0%, respectively) in calvarial defects ($p < 0.01$). Bone formation was only observed for the ErhBMP-2/bMBCP ectopic sites and was significantly greater at 8 wk (7.5%) than at 2 wk (4.5%) ($p < 0.01$). Appositional and endochondral bone formation was usually associated with a significant increase in fatty marrow at 8 wk. The bMBCP carrier showed no evidence of bioresorption.

Conclusion: ErhBMP-2/bMBCP induced significant bone formation in both calvarial and ectopic sites. Further study appears to be required to evaluate the relevance of the bMBCP carrier.

Chang-Sung Kim, DDS, PhD, Department of Periodontology, College of Dentistry, Yonsei University, 134 Shinchon-Dong, Seodaemun-gu, 120-752 Seoul, Korea
Tel: +82 2 2228 3186
Fax: +82 2 392 0398
e-mail: dentall@yuhs.ac
*Authors who contributed equally to this work

Key words: animal model; bone grafting; growth factors

Accepted for publication May 18, 2011

The carrier for bone morphogenetic proteins (BMPs) should serve as a scaffold for bone-forming cells and should be biocompatible to allow its replacement by newly formed bone without any adverse tissue response (1,2). Although the ideal carrier should be biodegradable, it should also be able to maintain its integrity for a certain time to allow sufficient maturation of the newly formed bone (3). The space-maintaining capacity is one of the critical factors of a BMP carrier for clinical bone formation and maturation (4–6). Until now, absorbable collagen sponge (ACS) has been considered as a promising carrier for BMP-induced bone-tissue engineering (7–9). However, ACS is less effective for the regeneration of bone defects, where tissue compression may hinder bone formation owing to the lack of space-providing capacity (4).

Macroporous biphasic calcium phosphate (MBCP) is a biphasic mixture of hydroxyapatite and tricalcium phosphate (60:40 ratio), which is used widely in periodontal regeneration and implant surgery (10). Micropores at the MBCP surface might serve as nucleation sites for biological apatite precipitation (10), and macropores may allow for the entrapment of recombinant human BMP-2 (rhBMP-2), which has a high affinity for calcium phosphates, providing space for the maturation of new bone (11). Histologic evaluation of the human sinus grafted using MBCP demonstrated excellent new bone formation and maturation on the surface and in the macropores of MBCP (12).

Many trials have addressed the production of biologically active rhBMPs in prokaryotic cells, such as *Escherichia coli*, as an alternative to the rhBMPs produced in mammalian cells (13–16). BMP-2 and BMP-4 have been produced successfully using *E. coli* systems, and their activities have been verified both *in vivo* and *in vitro* (14,15,17,18). Recently we produced a novel *E. coli*-expressed recombinant human BMP-2 (ErhBMP-2) that exhibits biological activity via the post-translational refolding technique, and we reported that ErhBMP-2 induced new bone formation at the ectopic site and markedly enhanced new bone formation at the orthotopic site in a dose-dependent manner using an ACS carrier (17,19). However, it also raised the question of whether ErhBMP-2 could induce more bone formation when used with a longer-lasting and highly space-maintaining carrier system, such as block-type MBCP (bMBCP).

The aim of the present study was to investigate ErhBMP-2-induced bone formation and maturation using a bMBCP with space-maintaining capacity, and to evaluate bMBCP as a carrier system for ErhBMP-2 in rat calvarial-defect and ectopic subcutaneous models.

Material and methods

Animals

Thirty-two male Sprague–Dawley rats (250–300 g in weight) were used. The rats were maintained in plastic cages in a 12-h day/12-h night cycle room at a temperature of 21°C. They were provided with water and standard feed pellets *ad libitum*. The animal selection, management, surgical protocols and preparations were in accordance with the guidelines approved by the Institutional Animal Care and Use Committee, Yonsei Medical Center (Seoul, Korea).

Expression and purification of ErhBMP-2

The ErhBMP-2 was produced at the Research Institute of Cowellmedi (Pusan, Korea), according to methods described previously (17). Briefly, total RNA from human osteosarcoma cells was reverse transcribed with reverse transcriptase (Gibco, Grand Island, NY, USA) into complementary DNA (cDNA) encoding the mature peptide of the BMP-2 protein. The cDNA was amplified using the PCR. The cDNA of mature BMP-2 was then subcloned into a pRSET(A) vector (Invitrogen, Paisley, UK) and pRSET(A)/hBMP-2 was used to transform the *E. coli* BL21(DE3) strain. Cells were cultured at a high density using a bioreactor (KoBioTec, Incheon, Korea), as described by Tabandeh *et al.* (20). The cultured biomass was harvested, and inclusion bodies (pellets) were obtained after passing the harvested cells through a French press. Post-translational glycosylation was not performed because previous research has shown that the basic glycosylated N-terminal domains of rhBMP-2 are not obligatory for receptor activation, and therefore post-translational glycosylation is not critical for functional ErhBMP-2 (18). The nonglycosylated ErhBMP-2 obtained was then refolded into its biologically active dimer form *in vitro*. After the purification procedure, the active protein of ErhBMP-2 could be eluted and separated.

ErhBMP-2 implant construction

The bMBCP disc implants (3 mm in height and 8 mm in diameter) were manufactured by Biomatlante (Vigneux de Bretagne, France). The micromorphologies of the bMBCP surfaces were evaluated using a scanning electron microscope (S-4300; Hitachi, Tokyo, Japan), and the distribution and size of the micropores were evaluated by micro-computed tomography (micro-CT; μ-CT80; Scanco Medical, Shenzhen, China) (Fig. 1). Scanning electron microscopy and micro-CT evaluation of the bMBCP scaffold showed that the macropores were interconnected and well distributed throughout the scaffold. The high-power observation revealed that micropores smaller than 5 μm were also well organized on the surface of the bMBCP. The pore sizes of the bMBCP varied from 35 μm to > 500 μm, with an average pore size of around 350 μm. Macropores of 250–450 μm were estimated to account for over 50% of all macropores. ErhBMP-2 was diluted in buffer to a concentration of 25 μg/mL. To produce ErhBMP-2/bMBCP implants, bMBCP implants were loaded with 0.1 mL of ErhBMP-2 solution 1 h before surgery.

Surgical procedures and experimental design

The rats were anesthetized by intramuscular injection (5 mg/kg body weight) of a 4:1 solution of ketamine hydrochloride (Ketalar; Yuhan, Seoul,

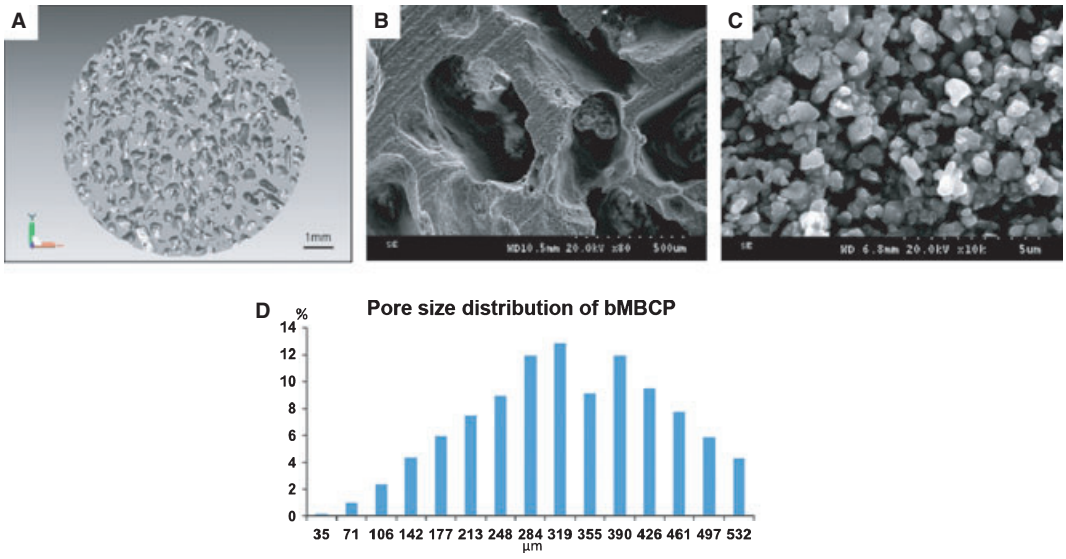

Fig. 1. Characterization of the block-type macroporous biphasic calcium phosphate (bMBCP) scaffold. (A) Micro-computed tomography (micro-CT) evaluation of bMBCP scaffolds showing interconnections among the macropores. (B and C) Scanning electron micrograph of the macropores and micropores of the bMBCP scaffolds (B, × 80 magnification; C, × 10,000 magnification). (D) Pore size distribution of bMBCP, evaluated using micro-CT images.

Korea) and xylazine (Rompun; Bayer Korea, Seoul, Korea).

To produce calvarial defects, an incision was made in the sagittal plane across the cranium. A full-thickness flap was reflected to expose the calvarial bone. A standardized, circular, transosseous defect, 8 mm in diameter, was created on the cranium using a saline-cooled trephine drill (Biomet 3i, Palm Beach Gardens, FL, USA), and the designated biomaterial was placed into the defects. The periosteum and skin were closed with an absorbable monofilament suture (Monosyn; Aesculap, Tuttlingen, Germany) for primary intention healing.

For the ectopic subcutaneous model, a vertical incision was made in the skin of the back. After flap reflection, a subcutaneous pocket was prepared with a blunt instrument. The skin was closed with an absorbable monofilament suture after implantation. The animals were divided into two groups of 16 animals each and they were allowed to heal for either 2 or 8 wk. Each rat received either the bMBCP carrier alone (bMBCP group) or ErhBMP-2/bMBCP (ErhBMP-2/bMBCP group) in both the calvarial-defect and ectopic-site subcutaneous models. Each rat had both a calvarial and an ectopic subcutaneous defect.

Histologic procedures and evaluation methods

At 2 or 8 wk after surgery, the rats were killed by CO_2 asphyxiation. Block sections that included the experimental sites were removed and fixed in 10% neutral-buffered formalin for 10 d. The samples were decalcified using 5% formic acid for 14 d and then embedded in paraffin. Serial, 7-μm-thick sections were cut and then stained using hematoxylin and eosin, Masson's trichrome and Safranin-O-fast green, and examined by optical and polarized microscopy (BX41 Laboratory Microscope; Olympus Optical, Tokyo, Japan). The most central section from each block was selected for histologic and histometric evaluation.

Computer-assisted histometric measurements were acquired using an automated image-analysis system (Image-Pro Plus; Media Cybernetics, Silver Spring, MD, USA) coupled with a video camera attached to an optical microscope. The sections were reviewed by one experienced masked examiner (C.S.K.) in duplicate to minimize intra-examiner errors and examined at magnifications of × 40 and × 400. Adipose tissue was separately stained using nondecalcified processing (data not shown), and the respective area was matched in hematoxylin and eosin-stained sections. The following histometric parameters were used for measurements (Fig. 2):

i Augmented area (mm^2): all tissues within the boundaries of the MBCP carrier (i.e. new bone, adipose tissue, fibrovascular tissue/marrow and residual biomaterial).
ii New bone area (mm^2): the area of newly formed bone within the total augmented area.
iii Adipose tissue area (mm^2): the area of newly formed adipose tissue within the total augmented area.
iv Residual material area (mm^2): the area of residual biomaterials within the total augmented area.

Statistical analysis

The histometric recordings from the samples were used to calculate means and standard deviations. Interactions between the healing period and the treatment condition were examined using two-way analysis of variance. An unpaired *t*-test was used for comparison between the two groups. The level of statistical significance was set at $p < 0.01$.

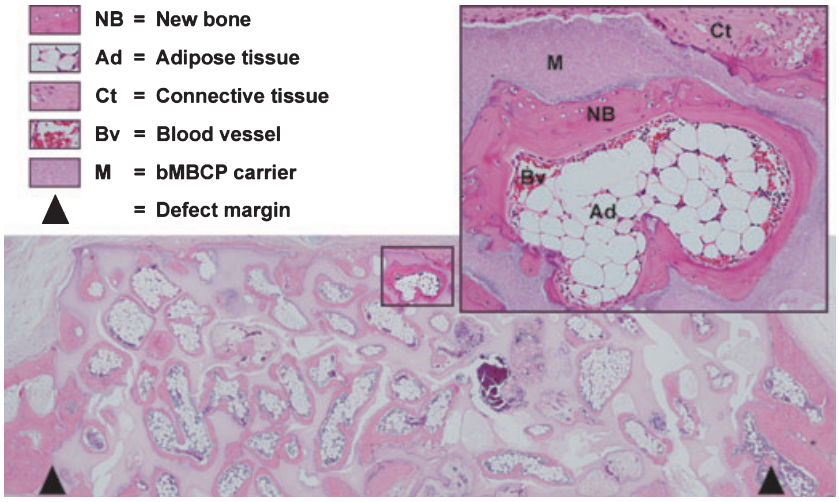

Fig. 2. Representative photomicrograph of the calvarial osteotomy defect showing histometric analysis.

Results

Bone formation and maturation in the rat calvarial-defect model

Clinical healing was generally uneventful. Material exposure or other complications at the surgical site were not observed. Two specimens from the calvarial defects of the bMBCP group at 2 wk and the ErhBMP-2/bMBCP group at 8 wk were respectively excluded for histologic inflammation of unknown etiology. Another two specimens from ectopic sites of ErhBMP-2/bMBCP groups at 2 and 8 wk, respectively, were excluded because of technical complications.

Histologic and histometric results from the calvarial-defect model are shown in Fig. 3 and Table 1. Volumetric tissue augmentation was achieved, and the total augmented area did not differ significantly between the 2- and 8-wk time-points in both groups, suggesting that the total augmented area was well maintained during the healing period.

In the bMBCP group, minimal new bone formation was observed adjacent to the defect margin and along the lower border of the bMBCP block at 2 wk postsurgery, and this was significantly enhanced at 8 wk ($p < 0.01$). The histologic results showed that the bone-forming activity was significantly enhanced only in the lower part of the bMBCP, and it appeared that most of the macropores in the lower part of the block had filled with newly formed bone. As the healing time increased, the specimens exhibited a more advanced stage of regeneration and consolidation of new bone.

In the ErhBMP-2/bMBCP group, there was evident bone-forming activity at 2 wk postsurgery, and it was significantly greater than that in the bMBCP group ($p < 0.01$). Most of the macropores in the lower and upper parts showed new bone tissues, including a dense osteoblast-like cell lining and osteoid tissue formation around the graft material. Active formation of new bone was also observed adjacent to the defect margin. Thus, the total augmented area was significantly larger than in the bMBCP group ($p < 0.01$), and this difference was maintained until 8 wk postsurgery. In the case of macropores, where increased bone-forming activity was observed, new bone was in direct contact with the surface of the bMBCP, and there was new bone formation inside the center of the macropore. The ErhBMP-2/bMBCP group exhibited a higher level of new bone formation than the bMBCP group and a greater quantity of new bone had been formed at 8 wk postsurgery than at 2 wk postsurgery ($p < 0.01$) in the ErhBMP-2/bMBCP group. This newly formed bone comprised woven and lamellar bone, and exhibited cement lines that were separated from the bone which had been deposited more recently. Overall, an 8-wk healing period yielded a more mature healing pattern of regeneration and consolidation, which was confirmed by Masson's trichrome staining and polarized light microscope observation (data not shown). However, abundant residual biomaterials were observed during the healing period, and largely remained unresorbed. Although the total area of residual bMBCP particles slightly decreased over the healing periods, this was not statistically significant.

Appositional bone growth represented a major healing pattern in both the bMBCP and ErhBMP-2/bMBCP groups. However, the additional association of endochondral bone formation was observed in the bMBCP group as well as in the ErhBMP-2/bMBCP group in very limited areas (Fig. 4). Chondrocytes and associated cartilage formation were more evident from the ErhBMP-2/bMBCP group after staining with Safranin-O-fast green, and an endochondral bone-formation pattern was increased in the 8-wk healing group of ErhBMP-2/bMBCP. Additionally, new bone formation in the ErhBMP-2/bMBCP group was associated with adipose tissue formation (Table 1). The ErhBMP-2/bMBCP group exhibited the largest and most statistically significant increase in the area of adipose tissue at the 8-wk healing point ($p < 0.01$). Among the newly formed bone, which had an advanced healing pattern (such as lamellation and cement lines), adipose tissue formation with blood-vessel insertion was a common finding. This phenomenon was initiated at 2 wk postsurgery and exhibited a more advanced pattern at 8 wk.

Bone formation and maturation in the rat ectopic subcutaneous model

Histologic and histometric results from the ectopic subcutaneous model are presented in Table 1 and Fig. 5. In the bMBCP group, bMBCPs were enclosed by loose connective tissue, and the macropores were permeated with connective tissue. Although some areas of the bMBCP group exhibited a dense collagen arrangement at 8 wk

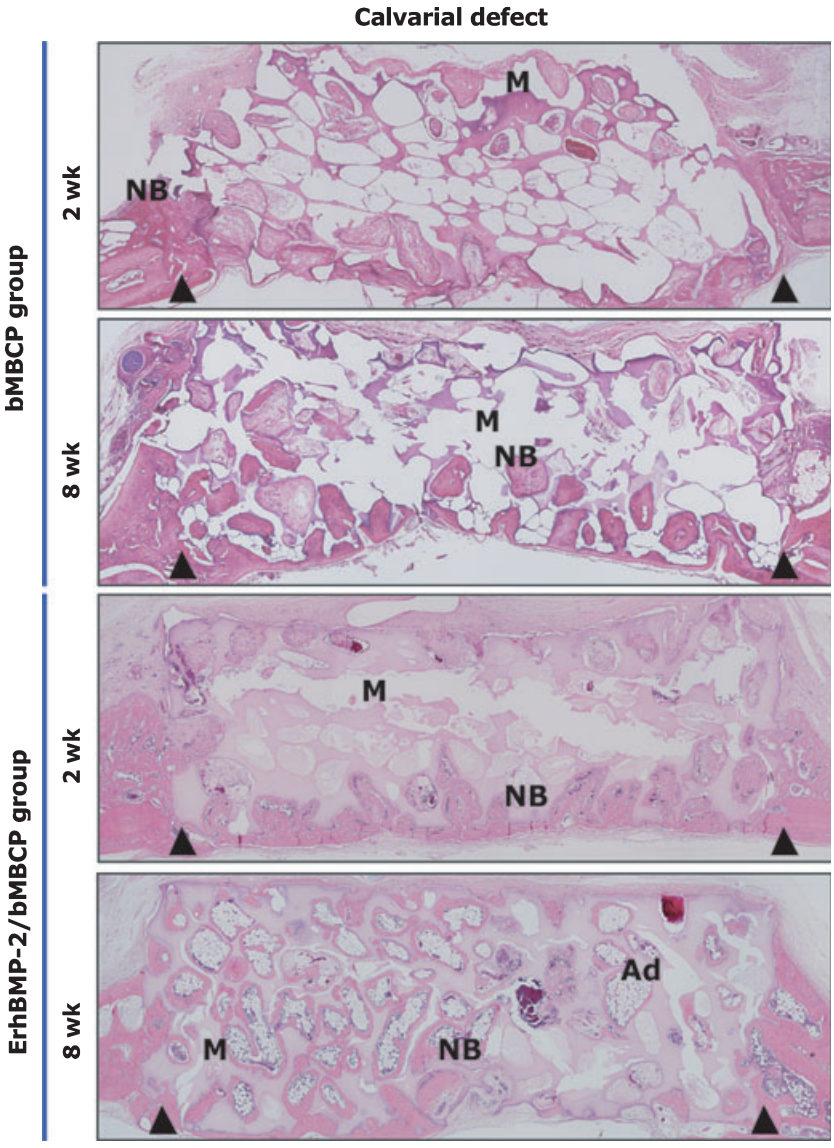

Fig. 3. Representative photomicrographs of calvarial-defect sites receiving block-type macroporous biphasic calcium phosphate (bMBCP) alone and *Escherichia coli*-expressed recombinant human bone morphogenetic protein-2 (ErhBMP-2)/bMBCP at 2 and 8 wk. In the bMBCP group, thin and loose connective tissue is observed in the macropores. However, new bone formation is found in the defect margins and along the lower border of the bMBCP. Mature bone appeared to be composed of woven bone and lamellar bone. In the ErhBMP-2/bMBCP group, active new bone formation and blood vessel insertion are evident. Distinguished lamellated patterns are observed at 8 wk, indicating the formation of fully matured bone. New bone was formed mainly by appositional bone formation, but endochondral bone formation was also involved in the both groups, especially in the ErhBMP-2/bMBCP group at 8 wk. Also, new bone formation at 8 wk was associated with adipose tissue formation when viewed at higher magnification (figure not shown). Arrow heads = defect margin. Ad, adipose tissue; M, bMBCP; NB, new bone. Hematoxylin and eosin stain; original magnification × 40).

postsurgery, there was no indication of osteogenic activity histologically.

In the ErhBMP-2/MBCP group, histologic findings at 2 wk postsurgery revealed active bone-forming activity at the periphery of the bMBCP, suggesting the osteoinductive potential of ErhBMP-2. The new bone or bone matrix appeared to be immature and was covered with cells that appeared to be osteoblasts. There was no evidence of significant adverse responses. The new bone formation was significantly enhanced at 8 wk postsurgery ($p < 0.01$), and the specimens exhibited a more advanced stage of new bone consolidation, including a dense osteoblastic cell lining, cement lines and Haversian systems, which was also confirmed by Masson's trichrome staining and polarized light microscope observation (data not shown). The number of specimens showing new bone induction increased from five to six. Adipose tissue formation could also be observed inside the macropores at 8 wk, while there was no indication of chondrocyte or cartilage formation under Safranin-O-fast green staining (Fig. 4). The total area of residual bMBCP particles slightly decreased but this was not statistically significant.

Discussion

The objective of the present study was to evaluate ErhBMP-2-induced bone formation and maturation using bMBCP and to evaluate bMBCP as a carrier for ErhBMP-2 in rat calvarial and ectopic-site defect models. The rationale behind this aim was to utilize the space-maintaining potential of bMBCP and to maximize the bone-forming activity of ErhBMP-2.

In the present study, ErhBMP-2 facilitated new bone-formation activity in both the calvarial-defect and ectopic-site models. These results are consistent with those of our previous study (19), which showed that ErhBMP-2 provoked osteoinductive and osteoconductive potential using an ACS carrier in the same defect models and with the same healing periods used in the present study. The potential of BMPs to induce new bone formation is crucially dependent upon the characteristics of the carrier (1,2). Space-maintaining capacity is one of the critical prerequisites for clinical bone formation and maturation. For example, ACS has been used as an effective carrier for rhBMP-2, but it does not exert its full capacity as a carrier at sites where the space-maintaining capacity could be disturbed by tissue compression (4). The effect of rhBMP-2/ACS

Table 1. Histomorphometric analysis of the calvarial defect and ectopic subcutaneous groups for block-type macroporous biphasic calcium phosphate (bMBCP) and *Escherichia coli*-expressed recombinant human bone morphogenetic protein-2 (ErhBMP-2)/bMBCP

	Calvarial defects		Ectopic site	
	2 wk	8 wk	2 wk	8 wk
Augmented area				
bMBCP	20.8 ± 2.5 (n = 7)	20.1 ± 2.1 (n = 8)	21.1 ± 2.3 (n = 8)	19.6 ± 2.8 (n = 8)
ErhBMP-2/bMBCP	23.1 ± 1.0[a] (n = 8)	24.0 ± 1.4[a] (n = 7)	22.3 ± 2.0 (n = 7)	22.6 ± 1.8 (n = 7)
New bone area				
bMBCP (%, n)	1.1 ± 0.6 (5.3, n = 7)	2.8 ± 0.8[b] (14.0, n = 8)	–(n = 8)	–(n = 8)
ErhBMP-2/bMBCP (%, n)	2.5 ± 1.1[c] (10.8, n = 8)	6.1 ± 1.5[b,c] (25.4, n = 7)	1.0 ± 0.5 (4.5, n = 7, n' = 5)	1.7 ± 0.8[d,e] (7.5, n = 7, n' = 6)
Adipocyte tissue area				
bMBCP (%, n)	0.02 ± 0.01 (0.1, n = 7)	0.08 ± 0.03 (0.4, n = 8)	–(n = 8)	–(n = 8)
ErhBMP-2/bMBCP (%, n)	0.06 ± 0.01 (0.3, n = 8)	7.27 ± 1.93[f] (30.3, n = 7)	–(n = 7)	0.92 ± 0.81[f] (4.1, n = 7)
Residual material area				
bMBCP (%, n)	10.6 ± 2.5 (51.0, n = 7)	9.3 ± 1.9 (46.3, n = 8)	10.1 ± 2.1 (47.9, n = 8)	9.6 ± 2.3 (49.0, n = 8)
ErhBMP-2/bMBCP (%, n)	9.3 ± 2.3 (40.3, n = 8)	8.9 ± 2.5 (37.1, n = 7)	9.8 ± 1.3 (44.0, n = 7)	9.2 ± 2.4 (40.7, n = 7)

[a]Statistically significant difference compared with the bMBCP group ($p < 0.01$).
[b]Statistically significant difference compared with 2 wk ($p < 0.01$).
[c]Statistically significant difference compared with the bMBCP group ($p < 0.01$).
[d]Statistically significant difference compared with 2 wk ($p < 0.01$).
[e]Statistically significant difference compared with the bMBCP group ($p < 0.01$).
[f]Statistically significant difference compared with the other groups ($p < 0.01$).
Data are given as group mean ± standard deviation (mm^2).
% = percentage of specific tissue in relation to the total augmented area; n, number of specimens involved in the histologic evaluation; n', number of specimens showing ectopic bone induction.

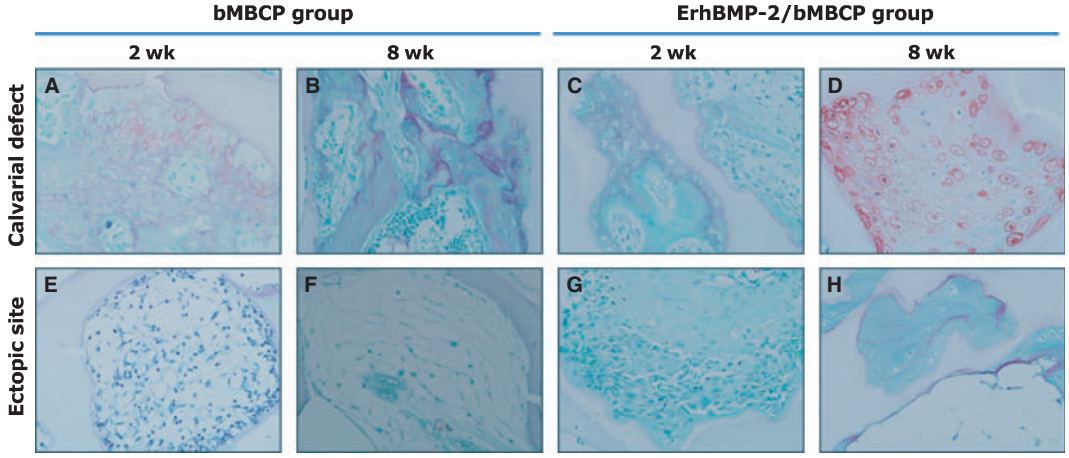

Fig. 4. Representative photomicrographs showing endochondral bone formation. Although appositional bone formation was mainly observed in both calvarial defect and ectopic sites, endochondral bone formation was also involved in calvarial defects, especially in the *Escherichia coli*-expressed recombinant human bone morphogenetic protein-2/block-type macroporous biphasic calcium phosphate (ErhBMP-2/bMBCP) group at 8 wk (Safranin-O-fast green stain; original magnification × 400).

was investigated on ridge augmentation in an alveolar bone ridge-defect model, and the results revealed limited augmentation by the implantation of rhBMP-2/ACS at 12 wk postsurgery, whereas sites receiving rhBMP-2/ACS combined with hydroxyapatite particles exhibited clinically relevant ridge augmentation (21).

Based on these observations resulting from the application of rhBMP-2/ACS, the authors hypothesized that a rigid type of carrier, such as bMBCP, would provide a greater space-maintaining effect, and the present study showed that bMBCP exerted a space-maintaining effect on new bone formation and maturation, unlike the

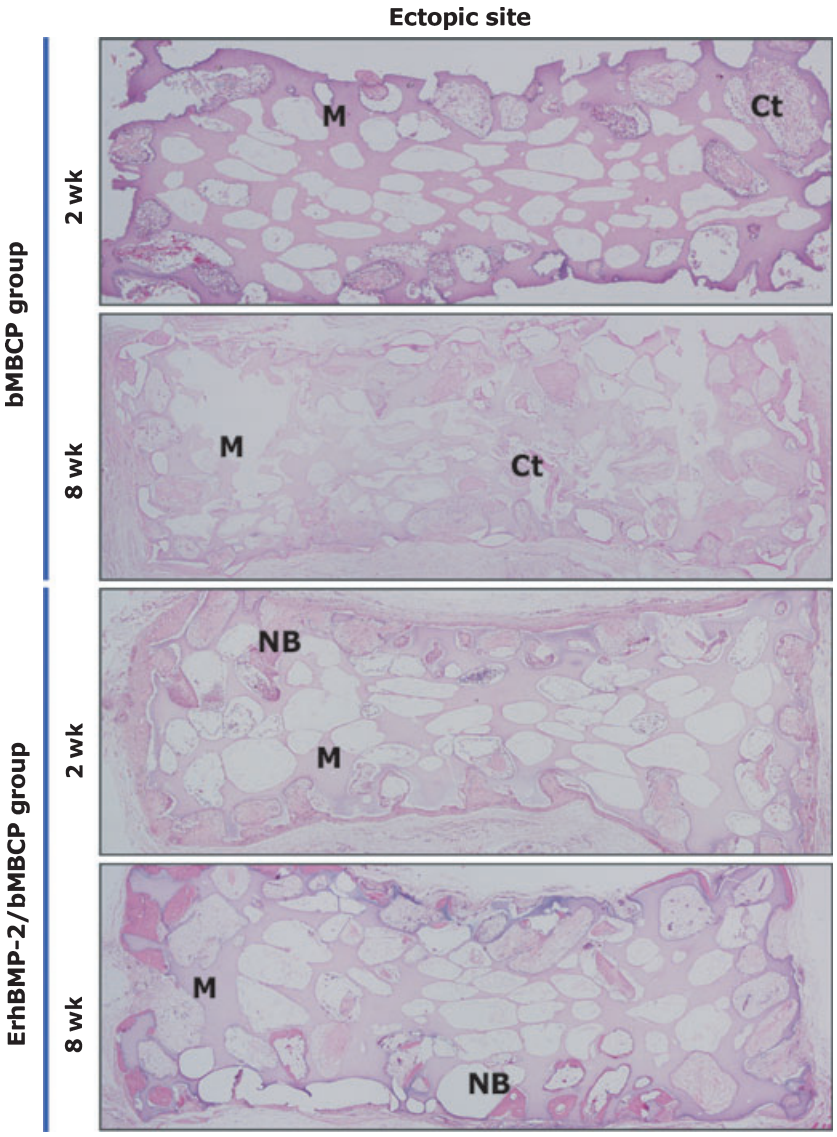

Fig. 5. Representative photomicrographs of ectopic sites receiving block-type macroporous biphasic calcium phosphate (bMBCP) alone and *Escherichia coli*-expressed recombinant human bone morphogenetic protein-2 (ErhBMP-2)/bMBCP at 2 and 8 wk. In the bMBCP group, thin and loose connective tissue healing is observed in the macropores. Evidence for ectopic bone induction could not be found, and there was no trace of woven or lamellated bone tissue. In the ErhBMP-2/bMBCP group, induction of new bone was evident at 2 wk, and advanced maturation of new bone was associated with adipose tissue formation at 8 wk. The apparent lamellation pattern demonstrated full maturation of newly formed bone at 8 wk. In the ectopic site, involvement of endochondral bone formation was a rare finding. Ct, connective tissue; M, bMBCP; NB, new bone. Hematoxylin and eosin stain; original magnification × 40.

ACS carrer. However, in contrast to previous studies, the total area of new bone tissue was generally limited, and residual material remained unresorbed for a long healing period. Possible mechanisms underlying limited new bone formation include the fact that unresorbed biomaterial probably restricted new bone ingrowth or that the current dose of ErhBMP-2 was too low for active new bone formation, although the dosage was determined based on the results of a previous study (19). Further studies are required to fully understand the possible mechanism related to this phenomenon.

At the ectopic site, enhanced bone maturation and increased numbers of specimens showing bone induction were observed in the late-healing group. This finding is comparable with the results of our previous study (19), in which new bone was observed in all specimens at 2 wk postsurgery using the ErhBMP-2/ACS system at the ectopic site. However, despite the maturation and degree of regeneration, some of the new bone had disappeared by 8 wk postsurgery. Interestingly, most of animals of the previous study did not exhibit new bone formation at 8 wk postsurgery in the ErhBMP-2/ACS group, which implies that early resorption of the scaffold ultimately interferes with further new bone formation.

In the present study, new bone was formed mainly through appositional bone formation in both groups. However, endochondral bone formation was also observed in the calvarial-defect model in both groups, while it was not observed at the ectopic site. These findings are consistent with those of a recently reported study which found that BMP-2 directed cell differentiation towards the chondrogenic lineage within the periosteum but not the endosteum (22). This suggests that osteogenic progenitor cells within the periosteum and endosteum respond differently to BMPs.

The healing pattern did not differ markedly between the bMBCP and ErhBMP-2/bMBCP groups. However, the latter was typified by adipose tissue formation with new bone maturation. Adipose tissue formation was initiated at 2 wk postsurgery, but was more pronounced at 8 wk, showing close contact with the bone tissue. This increase in formation of adipose tissue at the late stage of healing is consistent with the finding of Shockley *et al.* (23) that the expression of adipocyte-related genes is initiated at the early healing stage and gradually increases throughout maturation, whereas osteoblast-related genes are expressed in a temporal manner and down-regulated after the initiation of adipogenic differentiation. Although the induction of adipose tissue formation by rhBMP-2 application is a normal process usually observed

after a long healing period, a relative increase of adipogenic activity observed in ErhBMP-2/bMBCP group might be related to the microenvironment of this specific carrier. The exact mechanism underlying this phenomenon is not fully elucidated, and this issue should be addressed in a future study.

Whilst adipogenic activity has previously been observed in several studies evaluating rhBMP-2 bone formation and is regarded as part of the bone maturation process, little is known about the exact mechanism underlying BMP signaling in adipogenesis. Previously, a number of studies have shown that peroxisome proliferator-activated receptor gamma (PPARγ) plays an important role in the regulation of BMP-induced osteogenic and adipogenic differentiation. A recent comprehensive analysis of BMP indicated that several osteogenic BMPs exhibit strong adipogenic activity, which is regulated by the action of PPARγ2 (24). Decreased PPARγ2 activity causes increased bone density and an increased number of osteoblasts (25), while an increase in PPARγ2 activity following treatment with a PPARγ agonist resulted in a significant decrease in bone density, along with a decreased number of osteoblasts and an increased number of adipocytes (26,27). Therefore, future investigations should include the control of adipogenic differentiation to improve bone-tissue regeneration by rhBMP-2.

In conclusion, the findings of the present study confirm that ErhBMP-2 has osteoinductive potential and enhances the physiologic formation and maturation of new bone. Although a space-maintaining effect of bMBCP was demonstrated in this study, the amount of new bone formation was limited, probably because of the minimal resorption of biomaterials or the low dose of ErhBMP-2. Further studies are required to evaluate the relevance of bMBCP as a potential carrier for ErhBMP-2.

Acknowledgements

This study was supported by a grant from the Korea Healthcare Technology R &D Project, Welfare & Family Affairs, Korea (A084447). The authors would like to thank Ms Jae-Min Lee, web master, The One, Seoul, Korea for providing excellent graphic materials and data management.

Disclosure statement

No competing financial interests exist.

References

1. Seeherman H, Wozney JM. Delivery of bone morphogenetic proteins for orthopedic tissue regeneration. *Cytokine Growth Factor Rev* 2005;**16:**329–345.
2. Haidar ZS, Hamdy RC, Tabrizian M Delivery of recombinant bone morphogenetic proteins for bone regeneration and repair. Part A: current challenges in BMP delivery. *Biotechnol Lett* 2009;**31:**1817–1824.
3. Schliephake H, Weich HA, Dullin C, Gruber R, Frahse S. Mandibular bone repair by implantation of rhBMP-2 in a slow release carrier of polylactic acid – an experimental study in rats. *Biomaterials* 2008;**29:**103–110.
4. Kim CS, Kim JI, Kim J *et al*. Ectopic bone formation associated with recombinant human bone morphogenetic proteins-2 using absorbable collagen sponge and beta tricalcium phosphate as carriers. *Biomaterials* 2005;**26:**2501–2507.
5. Hong SJ, Kim CS, Han DK *et al*. The effect of a fibrin-fibronectin/beta-tricalcium phosphate/recombinant human bone morphogenetic protein-2 system on bone formation in rat calvarial defects. *Biomaterials* 2006;**27:**3810–3816.
6. Schwarz F, Rothamel D, Herten M, Ferrari D, Sager M, Becker J. Lateral ridge augmentation using particulated or block bone substitutes biocoated with rhGDF-5 and rhBMP-2: an immunohistochemical study in dogs. *Clin Oral Implants Res* 2008;**19:**642–652.
7. Boyne PJ, Lilly LC, Marx RE *et al*. De novo bone induction by recombinant human bone morphogenetic protein-2 (rhBMP-2) in maxillary sinus floor augmentation. *J Oral Maxillofac Surg* 2005;**63:**1693–1707.
8. Fiorellini JP, Howell TH, Cochran D *et al*. Randomized study evaluating recombinant human bone morphogenetic protein-2 for extraction socket augmentation. *J Periodontol* 2005;**76:**605–613.
9. Triplett RG, Nevins M, Marx RE. Pivotal, randomized, parallel evaluation of recombinant human bone morphogenetic protein-2/absorbable collagen sponge and autogenous bone graft for maxillary sinus floor augmentation. *J Oral Maxillofac Surg* 2009;**67:**1947–1960.
10. Le Nihouannen D, Guehennec LL, Rouillon T *et al*. Micro-architecture of calcium phosphate granules and fibrin glue composites for bone tissue engineering. *Biomaterials* 2006;**27:**2716–2722.
11. Le Nihouannen D, Saffarzadeh A, Gauthier O *et al*. Bone tissue formation in sheep muscles induced by a biphasic calcium phosphate ceramic and fibrin glue composite. *J Mater Sci Mater Med* 2008;**19:**667–675.
12. Lee JH, Jung UW, Kim CS, Choi SH, Cho KS. Histologic and clinical evaluation for maxillary sinus augmentation using macroporous biphasic calcium phosphate in human. *Clin Oral Implants Res* 2008;**19:**767–771.
13. Bessho K, Konishi Y, Kaihara S, Fujimura K, Okubo Y, Iizuka T. Bone induction by *Escherichia coli*-derived recombinant human bone morphogenetic protein-2 compared with Chinese hamster ovary cell-derived recombinant human bone morphogenetic protein-2. *Br J Oral Maxillofac Surg* 2000;**38:**645–649.
14. Kubler NR, Reuther JF, Faller G, Kirchner T, Ruppert R, Sebald W. Inductive properties of recombinant human BMP-2 produced in a bacterial expression system. *Int J Oral Maxillofac Surg* 1998;**27:**305–309.
15. Vallejo LF, Brokelmann M, Marten S *et al*. Renaturation and purification of bone morphogenetic protein-2 produced as inclusion bodies in high-cell-density cultures of recombinant *Escherichia coli*. *J Biotechnol* 2002;**94:**185–194.
16. Zhao M, Chen D. Expression of rhBMP-2 in *Escherichia coli* and its activity in inducing bone formation. In: Lindholm TS, ed. *Advances in Skeletal Reconstruction Using Bone Morphogenetic Proteins*. New Jersey: World Scientific, 2002:456.
17. Choi KH, Moon K, Kim SH, Yun JH, Jang KL, Cho KS. Purification and biological activity of recombinant human bone morphogenetic protein-2 produced by E. coli expression system. *J Korean Acad Periodontol* 2008;**38:**41–49.
18. Ruppert R, Hoffmann E, Sebald W. Human bone morphogenetic protein 2 contains a heparin-binding site which modifies its biological activity. *Eur J Biochem* 1996;**237:**295–302.
19. Lee JH, Kim CS, Choi KH *et al*. The induction of bone formation in rat calvarial defects and subcutaneous tissues by recombinant human BMP-2, produced in *Escherichia coli*. *Biomaterials* 2010;**31:**3512–3519.
20. Tabandeh F, Shojaosadati SA, Zomorodipour A, Khodabandeh M, Sanati MH, Yakhchali B. Heat-induced production of

human growth hormone by high cell density cultivation of recombinant *Escherichia coli*. *Biotechnol Lett* 2004;**26:**245–250.
21. Barboza EP, Duarte ME, Geolas L, Sorensen RG, Riedel GE, Wikesjo UM. Ridge augmentation following implantation of recombinant human bone morphogenetic protein-2 in the dog. *J Periodontol* 2000;**71:**488–496.
22. Yu YY, Lieu S, Lu C, Colnot C. Bone morphogenetic protein 2 stimulates endochondral ossification by regulating periosteal cell fate during bone repair. *Bone* 2010;**47:**65–73.
23. Shockley KR, Lazarenko OP, Czernik PJ, Rosen CJ, Churchill GA, Lecka-Czernik B. PPARgamma2 nuclear receptor controls multiple regulatory pathways of osteoblast differentiation from marrow mesenchymal stem cells. *J Cell Biochem* 2009;**106:**232–246.
24. Kang Q, Song WX, Luo Q *et al*. A comprehensive analysis of the dual roles of BMPs in regulating adipogenic and osteogenic differentiation of mesenchymal progenitor cells. *Stem Cells Dev* 2009;**18:**545–559.
25. Akune T, Ohba S, Kamekura S *et al*. PPARgamma insufficiency enhances osteogenesis through osteoblast formation from bone marrow progenitors. *J Clin Invest* 2004;**113:**846–855.
26. Ali AA, Weinstein RS, Stewart SA, Parfitt AM, Manolagas SC, Jilka RL. Rosiglitazone causes bone loss in mice by suppressing osteoblast differentiation and bone formation. *Endocrinology* 2005;**146:**1226–1235.
27. Soroceanu MA, Miao D, Bai XY, Su H, Goltzman D, Karaplis AC. Rosiglitazone impacts negatively on bone by promoting osteoblast/osteocyte apoptosis. *J Endocrinol* 2004;**183:**203–216.